analytical chemistry

pubs.acs.org/ac Article

Intensive and Persistent Chemiluminescence System Based on Nano-/Bioenzymes with Local Tandem Catalysis and Surface Diffusion

Pengyun Dang,[§] Xuan Liu,[§] Huangxian Ju, and Jie Wu*

Cite This: *Anal. Chem.* 2020, 92, 5517−5523 Read Online

ACCESS | Metrics & More | Article Recommendations | Supporting Information

ABSTRACT: A chemiluminescence (CL) system with long persistent and intensive emission is essential for accurate CL quantitative analysis and imaging assay. However, with most known CL systems being flash-type, it is still a great challenge to develop long-lasting CL systems. Here, by combining an iron porphyrin metal−organic frameworks (FePorMOFs) based peroxidase mimic with natural glucose oxidase (GOx), an intensive and persistent CL system is presented on the basis of local tandem catalysis and surface diffusion of the nano-/bioenzymes (FePorMOF/GOx). FePorMOF synthesized by iron porphyrin linker and zirconium ion node possesses high peroxidase catalytic activity and stability. Using luminol and glucose as substrate, the FePorMOF/GOx CL system can produce intensive CL emission containing a plateau period of 7.5 h. The strong CL signal is due to the local tandem generation and reaction of H_2O_2 by GOx and FePorMOF, which avoids the diffusion-limited kinetics and leads to a high catalytic efficiency of the nano-/bioenzymes. On the other hand, the long persistent CL emission is attributed mainly to the enzymatic reaction-controlled H_2O_2 supply and surface diffusion-controlled CL reaction. The proposed CL system is explored for CL imaging sensing of glucose and homogeneous immunoassay of α-fetoprotein. The nano-/bioenzymes CL system exhibits intensive and long constant CL emission in physiological condition, showing promising applications in real-time bioassay and bioimaging.

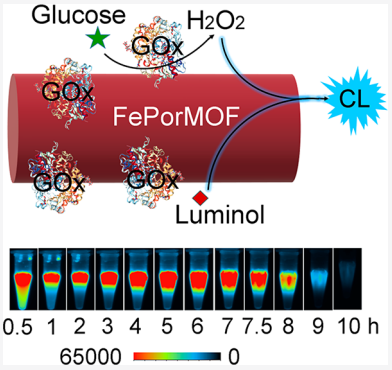

As chemiluminescence (CL) is excited by chemical reactions rather than excimer sources such as lasers and power supplies, it possesses advantages of high sensitivity, simple instrument, easy operation, and low cost and has been applied widely in chemical and biological fields.[1,2] Especially, CL has attracted attention in imaging analysis because it performs at a high signal-to-background ratio owing to no interferences of light source and autofluorescence.[3−5] At present, the most developed and used CL systems are enzyme-involved CL reactions, including luminol−oxidant−horseradish peroxidase (HRP)[6,7] and dioxetane−alkaline phosphatase (ALP)[8] CL systems. However, the CL intensity and emission time of these enzyme based CL systems suffer from the poor stability and difficult modification of natural enzymes, limiting their application in bioimaging assays.

Besides, the peroxyoxalate ester CL system[3,9−11] and Schaap's dioxetane CL system[5,12−14] have been designed to produce intensive and glow-type CL emission for in vivo imaging analysis. The former relies on the oxidation of peroxyoxalate esters with hydrogen peroxide (H_2O_2) to produce electronically excited 1,2-dioxetanedione intermediates which subsequently transfer energy to the fluorophore for luminescence. In order to achieve strong and long-lasting CL emission, different nanoparticles aggregating oxalate and fluorophore have been prepared. However, the lifetime of these CL nanoparticles (NPs) is only tens of minutes. The Schaap's dioxetane CL system is based on the chemiexcitation of adamantylidene−dioxetane through the removal of a protecting group by response molecules. In this case, because the CL efficiency of Schaap's dioxetane is extremely low in aqueous conditions, phenoxy−dioxetane or dioxetane−fluorophore probes should be synthesized for bioassay.

Recently, glow-type micro-/nanomaterial based CL systems also have been proposed with slow-diffusion-controlled heterogeneous catalytic mechanism. In this kind of CL system, a porous micro-/nanomaterial embedded with catalyst (and one CL reagent) is required.[15,16] The porous structure of the micro-/nanomaterial causes the slow diffusion of CL reagent (or the co-reactant), leading to the long-lasting CL emission. In addition, the high loading amount of catalyst in micro-/nanomaterials results in the strong CL signal. The most typical example is the chitosan hydrogel doped with CL reagent *N*-(4-aminobutyl)-*N*-ethylisoluminol and catalyst Co^{2+}, which can

Received: January 22, 2020
Accepted: March 20, 2020
Published: March 20, 2020

https://dx.doi.org/10.1021/acs.analchem.0c00337
Anal. Chem. 2020, 92, 5517−5523

exhibit a visible luminescence with hundreds of hours duration.[17] Although the CL emission of these CL systems can last for a few to hundreds of hours, the light intensity exhibits a peak shape change with duration time without a plateau period, which is imperfect for CL assay, especially for real-time bioimaging analysis.

Nanozymes referring to a kind of nanomaterials with enzymatic activity have been used widely in bioassay due to their charming feature of environmental tolerance over natural enzymes.[18,19] Among them, the peroxidase nanozymes are well developed, including various inorganic NPs[20] and the hemin functionalized nanomaterials.[21] Besides, metal−organic frameworks (MOFs) based peroxidase mimics have also been prepared by using an active center as a node. MOF exhibits high catalytic activity because each active center in MOF can exist in the form of monomer and its active site is accessible by substrates due to the inherent rigid and porous structure of MOF. Except for the applications in biomimetic catalysis, drug delivery, photodynamic therapy, and biosensing,[22−25] MOFs have also been used to catalyze CL systems.[26−28] Unfortunately, the MOFs-based CL systems show flash-type emission.

In this work, by combining iron porphyrin MOF (FePorMOF) with natural glucose oxidase (GOx), a dual nano-/bioenzymes design is proposed to develop the intensive and persistent CL system. The bi-enzyme system in which the substrate of one enzymatic reaction is produced in situ by another exists widely in organisms to carry out physiological processes. Particularly when the two enzymes are confined within a nanoscale range, the overall efficiency of enzymatic reactions can be remarkably amplified by reducing the diffusion barrier.[29−31] For example, by modifying both HRP and GOx on a quantum dot, a bi-enzyme−quantum dot conjugate has been prepared for enhancing the chemiluminescence resonance energy transfer efficiency and extending the luminous time to 1 h.[32] The presented dual nano-/bioenzymes are fabricated by direct adsorption of GOx on FePorMOF with high peroxidase catalytic activity. In the presence of luminol and glucose, H_2O_2 is generated in situ by GOx and consumed immediately by FePorMOF for the CL reaction. The local tandem catalytic reactions by FePorMOF/GOx avoid the diffusion-limited kinetics and enhance the overall catalytic efficiency, leading to a strong CL intensity. In addition, the in situ enzymatic production of H_2O_2 along with the surface diffusion effect makes the nano-/bioenzymes based CL system exhibit a long persistent CL emission with a plateau period of 7.5 h. On the basis of this CL system, CL imaging analysis methods have been successfully constructed for glucose sensing and homogeneous real-time immunoassay of α-fetoprotein (AFP). The proposed nano-/bioenzymes based CL system shows advantages of intensity, long persistence, and good biocompatibility and stability, making it a good detection tool for biosensing and bioimaging assay.

EXPERIMENTAL SECTION

Materials and Reagents. $ZrCl_4$ and *N*,*N*-dimethylformamide (DMF) were purchased from Aladdin Biochemical Technology Co., Ltd. (Shanghai, China). Fetcpp was obtained from Frontier Scientific (USA). GOx, thrombin, HRP, *N*-hydroxysuccinimide (NHS), and *N*-(3-(dimethylamino)-propyl)-*N*′-ethylcarbodiimide hydrochloride (EDC) were purchased from Sigma-Aldrich Co., Ltd. (Shanghai, China). Glucose and pyrogallol were purchased from Macklin Biochemical Technology Co., Ltd. (Shanghai, China). GOx assay kit (Fluorometric) was obtained from Abcam (Shanghai China). Luminol (∼2 mM) was provided by Autobio Diagnostics Co. Ltd. (Zhengzhou, China). AFP and corresponding antibodies (clone nos. Ab1 9K5# and Ab2 102 K7#) were purchased from Keybiotech Co. Ltd. (Beijing, China). All other reagents were of analytical grade and used without further purification.

Apparatus. The scanning electron microscopy (SEM) images were obtained by a JSM-7800F scanning electron microscope (JEOL Ltd., Japan). Powder X-ray diffraction (PXRD) patterns were obtained using a D8 ADVANCE XRD instrument (Bruker AXS, Germany). Fourier transform infrared (FTIR) spectra were acquired on a Nicolet 6700 spectrometer (Thermo Fisher Scientific, USA). UV−vis absorption values were obtained on a Varioskan Flash spectral scanning multimode reader (Thermo Fisher). ζ potential and dynamic light scattering (DLS) analysis were performed on 90 Plus/BI-MAS equipment (Brookhaven Instruments Co., USA). CL spectra and fluorescence measurements were performed on an F-7000 fluorescence spectrophotometer (Hitachi, Japan). The CL kinetics curves were obtained by an MPI-A multifunctional electrochemical and chemiluminescent analytical system (Xi'an Remex Analytical Instrument Co., Ltd. China) with a PMT 300. The CL images were collected through a cooled low-light CCD camera (BioSpectrum 615 Imaging System, UVP, USA). For image analysis, a square was first defined with side length around each spot center and then the mean pixel intensity within the square was used for the CL intensity calculation.

Synthesis of FePorMOF. FePorMOF was synthesized according to previous work with little modification.[33] Briefly, 15 mg of $ZrCl_4$, 20 mg of Fetcpp, and 0.4 mL of CH_3COOH were dissolved in 5 mL of DMF with ultrasound. Then the mixture was heated at 120 °C for 12 h in a reaction kettle. After cooling to room temperature, the brown solid FePorMOF was obtained through centrifugation, washing with DMF, and subsequent drying under vacuum at 60 °C for 24 h. The obtained FePorMOF was stored away from light.

Preparation of FePorMOF/GOx. The FePorMOF/GOx was prepared by mixing 1 mg/mL FePorMOF and 5 mg/mL GOx aqueous solution in equal volume, followed with slight shaking at room temperature for 12 h. After centrifugation washing, the FePorMOF/GOx was dispersed in ultrapure water and stored at 4 °C away from light for further use.

Fabrication of FePorMOF/Ab1/BSA. By considering the fabrication universality for different antibodies, FePorMOF/Ab1/BSA was prepared by covalent bonding. First, 1 mg/mL FePorMOF was reacted with the mixture of 0.4 M EDC and 0.1 M NHS for 1 h to activate the carboxyl group on its surface. After washing, 1 mg/mL activated FePorMOF was reacted with 1 mg/mL Ab1 (capture antibody of AFP) for 12 h at room temperature with slight shaking. Then FePorMOF/Ab1 was washed and blocked with BSA (5 mg/mL) for 12 h at room temperature with slight shaking. After centrifugation washing, FePorMOF/Ab1/BSA was obtained and stored at 4 °C away from light before use. Here, PBS (10 mM, pH 7.4) was used for washing, reaction, and storage.

Catalytic Activity Test. According to the previous works,[34,35] pyrogallol-H_2O_2 reaction was used to evaluate the peroxidase-like catalytic activity of Fetcpp and FePorMOF. The catalytic reaction was carried out with 4 μg/mL (5 μM) Fetcpp or 6 μg/mL (the active sites were equivalent to 5 μM Fetcpp) FePorMOF at different concentrations of pyrogallol

https://dx.doi.org/10.1021/acs.analchem.0c00337
Anal. Chem. 2020, 92, 5517−5523

(Fetcpp, 5, 10, 20, 25, and 40 mM; FePorMOF, 5, 10, 15, 20, and 35 mM) and 10 mM H_2O_2. The increase of the product absorbance in the first 50 s was monitored by UV−vis spectroscopy at 420 nm in the kinetic mode with 2 s intervals. The reaction progress followed a conventional enzymatic dynamic regulation expressed by Michaelis−Menten equation. The Michaelis constant K_M and catalytic constant K_{cat} were calculated by the Lineweaver−Burk plot (eq 1).

$$\frac{1}{V} = \frac{K_M}{V_{max}}\frac{1}{[S]} + \frac{1}{V_{max}} \quad (1)$$

Glucose Detection. Glucose of different concentrations was mixed with FePorMOF/GOx and luminol in which the final concentrations of FePorMOF/GOx and luminol were 0.2 mg/mL and 0.8 mM, respectively. The mixture was added in a 96-well plate and immediately used for CL image collection by CCD with an exposure time of 15 min.

AFP Detection. AFP of different concentrations were mixed with the reaction solution containing 0.1 mg/mL FePorMOF/Ab1/BSA, 0.1 μg/mL Ab2, 0.25 μg/mL GOx, 0.4 mM luminol, and 5 mM glucose. The mixture was added in a 96-well plate and immediately used for continuous CL image collection by CCD. Each CL image was recorded with an exposure time of 10 min.

RESULTS AND DISCUSSION

Nano-/Bioenzymes Based CL System. The principle of the nano-/bioenzymes CL system using FePorMOF/GOx bioconjugate was illustrated in Figure 1A. In the presence of glucose, H_2O_2 was in situ generated by GOx and then immediately oxidized luminol with FePorMOF to emit blue light. The FePorMOF/GOx bioconjugate could confine the CL reaction on the local surface of FePorMOF via the cascaded H_2O_2 generation and consumption. Because the nano-/bioenzymes CL system evaded the diffusion-limited kinetics, the overall catalytic efficiency was amplified to generate strong CL emission over 9 h (Figure 1B). In addition, the image analysis showed the nano-/bioenzymes system could emit strong luminescence initially and the intensity would maintain at the plateau value over 7.5 h (Figure 1C). Such persistent CL emission with a long plateau period of several hours should be mainly attributed to the controlled H_2O_2 supply by the in situ enzymatic reaction.[32]

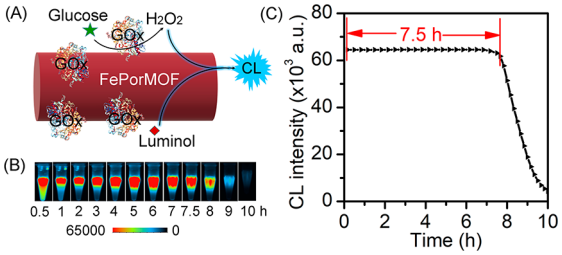

Figure 1. (A) Schematic principle of the FePorMOF/GOx based CL system, (B) CL emission, and (C) corresponding image analysis of 0.1 mg/mL FePorMOF/GOx with 1.2 mM luminol and 5 mM glucose.

The kinetic curve of the CL reaction of FePorMOF/GOx, luminol, and glucose illustrated that the CL intensity of the proposed nano-/bioenzymes system underwent four stages: (I) rapid rise to the peak value, (II) fall to the plateau, (III) long lasting at plateau, and (IV) decay to background (Figure 2). The behavior of this kinetic curve should be attributed to both

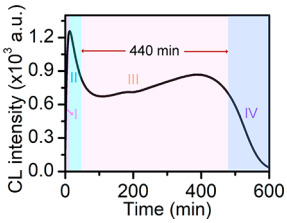

Figure 2. Kinetic curve of the CL reaction of 0.1 mg/mL FePorMOF/GOx with 1.2 mM luminol and 5 mM glucose.

the enzymatic reaction kinetics and substrate diffusion kinetics. In stage I, since the concentrations of both luminol and glucose around FePorMOF/GOx were consistent with their bulk concentrations, the cascaded enzymatic reactions were mainly carried out to generate strong CL; thus, the CL intensity increased rapidly to a peak. Due to the complete consumption of luminol and glucose, the substrates around FePorMOF/GOx should be supplied by diffusion from the bulk solution. Thus, in stage II the concentrations of substrates were lower than those in stage I; hence, the CL intensity fell from the peak. When the diffusion kinetics and enzymatic reaction kinetics reached equilibrium, a plateau was obtained (stage III). The kinetic curve showed a plateau for 440 min, which was consistent with 7.5 h of the image analysis results (Figure 1C). With the passage of time, luminol was gradually used up, leading to the decay of CL (IV). The exhaustion of luminol was verified by the recovery of CL intensity with extra addition of luminol (data not shown).

Characterization of FePorMOF. FePorMOF was synthesized by using Fetcpp as linker and zirconium ion as node via solvothermal reaction (Figure 3A). The SEM image showed the as prepared FePorMOFs were uniform in a rod-like structure with a 600 nm length and 150 nm width (Figure 3B). One thing to be noted, some FePorMOF surface had flakes; they should be from the uneven growth of MOF because the heating and cooling process would not be uniform absolutely. The FTIR characterization of FePorMOF showed the typical porphine ring skeleton absorptions at 1714 (w), 1606 (s), and 1419 (vs), and the O−H stretch absorption at 999 (s), indicating the involvement of Fetcpp in the frameworks (Supporting Information Figure S1A). Additionally, the PXRD curve showed the peaks at 4.87°, 7.15°, 8.30°, and 9.69°, which could be indexed to (−220), (410), (500), and (−150) of the spindle hexahedron geometry, respectively (Figure S1B).[33] All of the above results confirmed the successful synthesis of FePorMOF.

The CL generation of luminol-H_2O_2 by FePorMOF was studied. The CL spectra showed the emission peaks of luminol-H_2O_2 catalyzed by FePorMOF, Fetcpp, and HRP were all at 423 nm (Figure 3C). This result indicated the CL mechanism of luminol-H_2O_2-FePorMOF was similar to that of luminol-H_2O_2-HRP, in which FePorMOF catalyzed the oxidization of luminol to generate luminescence.

The catalytic parameters of FePorMOF and Fetcpp[36] were measured through the oxidation reaction of pyrogallol-H_2O_2. The Michaelis constant K_M of 3.20 mM and the catalytic constant K_{cat} of 4.99 min^{-1} were obtained for FePorMOF from the Lineweaver−Burk plot (Figure 3D and Table S1). Compared with Fetcpp, the FePorMOF processed a higher

https://dx.doi.org/10.1021/acs.analchem.0c00337
Anal. Chem. 2020, 92, 5517−5523

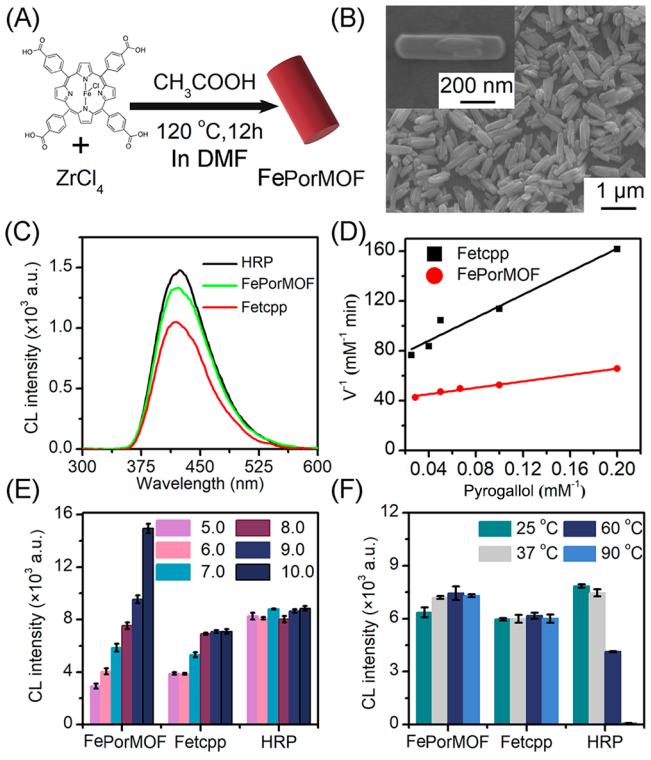

Figure 3. (A) Synthetic route and (B) SEM image of FePorMOF, (C) CL spectra, (D) Lineweaver–Burk plots of pyrogallol oxidation catalyzed by FePorMOF (6 μg/mL) and Fetcpp (4 μg/mL) in the presence of 10 mM H_2O_2, (E) pH and (F) temperature effects on CL intensity of luminol-H_2O_2 reaction catalyzed by FePorMOF, Fetcpp, and HRP. The concentrations of luminol, H_2O_2, and FePorMOF (in panels C, E, and F) were 0.08 mM, 1 mM, and 25 μg/mL.

K_{cat} value and lower K_M value, indicating its higher catalytic activity and affinity. The higher K_{cat}/K_M value also indicated the higher catalytic efficiency of FePorMOF than Fetcpp which might be due to the rigid and porous structure of MOF. FePorMOF could also be used for H_2O_2 detection because of its good catalytic ability (Figure S2).

The environmental tolerance of the catalytic ability was an important criterion of the enzyme. Here, the effects of pH and temperature on the catalytic activity of FePorMOF were investigated (Figure 3E,F). For FePorMOF, the CL intensity gradually increased when the pH of the reaction solution changed from acidic to alkaline (Figure 3E). This was because FePorMOF could maintain its activity in alkaline solution, which was more suitable for the luminol-H_2O_2 reaction.[37] However, for both Fetcpp and HRP CL systems, no significant change of CL intensity was observed when pH was higher than 8.0, indicating the partial loss of catalytic activity of Fetcpp and HRP in alkaline solution. One thing to be noted, the color of Fetcpp stock solution would change visually in alkaline solution due to the structural failure of Fetcpp. The temperature tolerance experiment showed both FePorMOF and Fetcpp could retain their activity even at 90 °C. In contrast, HRP was extremely sensitive to temperature; it would lose 48% activity at 60 °C and completely deactivate at 90 °C (Figure 3F). All of the above results indicated the higher stability of FePorMOF nanozyme than the natural HRP in alkaline and high-temperature environment.

Preparation of FePorMOF/GOx. FePorMOF/GOx bioconjugate was fabricated by electrostatic adsorption of electronegative GOx on the electropositive surface of FePorMOF. The hydration diameter analysis showed both FePorMOF and FePorMOF/GOx had two peak positions which were attributed to the horizontal and longitudinal diameter of the rod-like structure (Figure 4A). The two peaks of FePorMOF were at 140 and 532 nm, which was consistent with the result in SEM. In contrast to FePorMOF, the hydration diameters of FePorMOF/GOx extended to 160 and 541 nm, indicating the modification of GOx on the surface of FePorMOF. Meanwhile, the ζ potential experiment confirmed the electronegativity and electropositivity of GOx and FePorMOF (Figure 4B). Compared to the ζ potential of 54.6 mV of FePorMOF, the ζ potential of FePorMOF/GOx fell to 1.7 mV, confirming the modification of GOx on FePorMOF.

The modification amount of GOx on FePorMOF was calculated by GOx detection kit (Figure 4C). By subtracting the FL intensity of the supernatant solution after adsorption from the FL intensity of the GOx reaction solution, 0.92 mg of GOx was calculated to be absorbed on 1 mg of FePorMOF. This modification capacity was comparable to the direct physical encapsulation.[38]

Adjustment of the CL Duration Time. The persistent time of the CL system is significant for CL bioassay and imaging. In the present work, the nano-/bioenzymes system used glucose and luminol as substrates. Since the physiological concentration of glucose was ∼5 mM, the CL emission of FePorMOF/GOx-glucose-luminol was examined at different luminol concentrations with 5 mM glucose. The CL images showed the FePorMOF/GOx-glucose-luminol system could express strong emission to achieve the CCD exposure intensity threshold even with 0.2 mM luminol, and the CL duration time extended from 160 to 460 min with increasing luminol concentration from 0.2 to 1.2 mM (Figure 5A). Except the whole CL lasting time, the corresponding image intensity

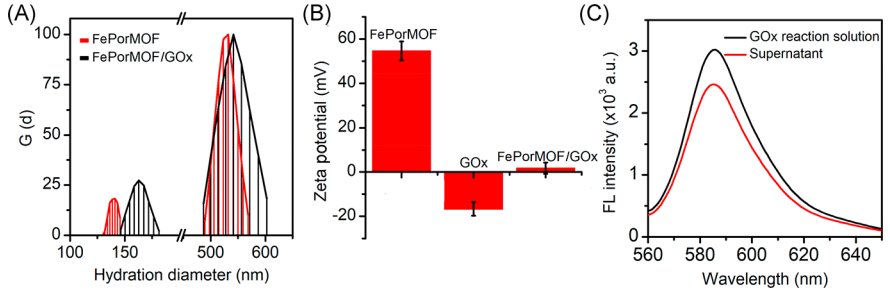

Figure 4. (A) Hydration diameter, (B) ζ potential characterization, and (C) FL intensity of the GOx reaction solution (5 mg/mL) and supernatant detected by the GOx kit.

https://dx.doi.org/10.1021/acs.analchem.0c00337
Anal. Chem. 2020, 92, 5517−5523

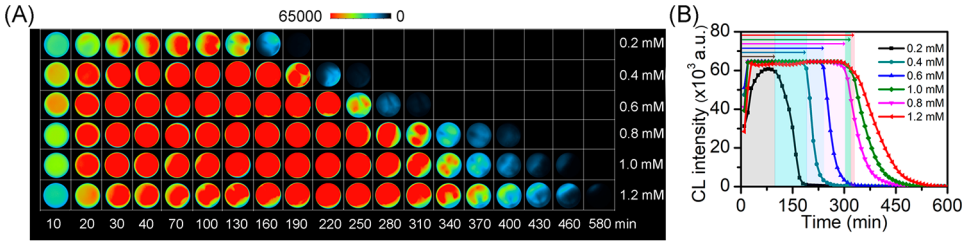

Figure 5. (A) CL imaging and (B) image intensity analysis of FePorMOF/GOx (0.1 mg/mL) triggered CL in the presence of 5 mM glucose and luminol of different concentrations.

analysis showed the plateau period also increased with increasing luminol concentration (Figure 5B). The adjustment of the CL duration time was also examined with the kinetic curves (Figure S3), which showed the CL emission possessed plateau periods in all luminol concentrations and the plateau period extending with the increase of luminol concentrations. These results indicated the CL persistent time, along with the plateau period, of the FePorMOF/GOx-glucose-luminol system could be adjusted by luminol concentrations. However, because the alkalinity of reaction solution would increase with the increase of luminol concentration, a relatively low luminol concentration of 0.4 mM used in the following experiments if there was no special explanation.

Persistent CL Performance. The CL performance of the proposed FePorMOF/GOx-glucose-luminol was compared with other CL systems using nonlocal bi-enzymes or H_2O_2 substrate (Figure 6). In this experiment, the glucose used was

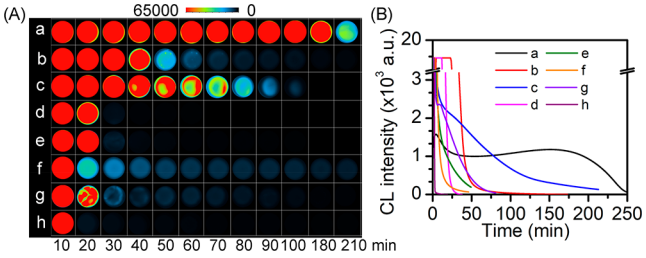

Figure 6. (A) CL imaging and (B) kinetic curves of (a) FePorMOF/GOx + glucose + luminol, (b) FePorMOF/GOx + luminol + H_2O_2, (c) FePorMOF + GOx + glucose + luminol, (d) FePorMOF + H_2O_2 + luminol, (e) Fetcpp + GOx + glucose + luminol, (f) Fetcpp + H_2O_2 + luminol, (g) HRP + GOx + glucose + luminol, and (h) HRP + H_2O_2 + luminol CL systems. The concentrations of luminol, H_2O_2, glucose, GOx, FePorMOF/GOx, FePorMOF, Fetcpp, and HRP were 0.4 mM, 10 mM, 5 mM, 1 mg/mL, 0.1 mg/mL, 0.1 mg/mL, 0.07 mg/mL, and 10 μg/mL.

at the physiological concentration of 5 mM, and the luminol used was at 0.4 mM, assuring the luminol could be all oxidized for luminescence. The CL images showed the CL duration time of the proposed FePorMOF/GOx-glucose-luminol system (a) was 210 min, which would be decreased to 50 or 80 min when using directly the H_2O_2 (b, FePorMOF/GOx-luminol-H_2O_2) or nonlocal bienzymes (c, FePorMOF-GOx-glucose-luminol) (Figure 6A). This was because the FePorMOF/GOx-glucose-luminol system could not only make the H_2O_2 production controlled by enzyme reaction but also make the H_2O_2-luminol reaction controlled by the diffusion, leading to the continuous oxidization of luminol for long persistent CL. In addition, the CL duration time of the FePorMOF-H_2O_2-luminol system (d) was 20 min, which was much shorter than the 50 min of FePorMOF/GOx-luminol-H_2O_2. This should be attributed to the hindrance of GOx on FePorMOF, confirming the slower catalytic CL reaction could lead to longer CL duration time. The extension of CL emission time by in situ enzymatic H_2O_2 production was also observed in Fetcpp (e) and HRP (g) based CL systems; however, in these systems the two catalyst were molecules, and thus, the CL duration time could only be 20 min due to the lack of diffusion control of the homogeneous CL reaction.

The kinetic curves also confirmed only the proposed FePorMOF/GOx-glucose-luminol system (a) could possess a persistent CL emission with long plateau period (Figure 6B). Assuming all enzymes had 100% reaction efficiency, the total photons should be the same in all of these systems due to the same amount of luminol. The kinetic curves showed all of the H_2O_2 triggered CL reactions, presenting a fast fading CL performance; however, the attenuation velocity of the FePorMOF system was lower than those of Fetcpp and HRP, indicating FePorMOF was a suitable catalyst for developing glow-type CL. In contrast, all of the bi-enzyme CL systems presented a relaxation luminescence, indicating the in situ H_2O_2 production could delay the oxidization of luminol for luminescence. All of the results indicated, on the basis of the local double enzyme design, the FePorMOF/GOx performed as an excellent persistent CL system with long plateau period through controlling the oxidization of luminol by both enzymatic reaction and substrate diffusion.

Stability of FePorMOF/GOx. The stability of FePorMOF/GOx was examined through FePorMOF/GOx-glucose-luminol CL system. In this experiment, the mixture of 0.1 mg/mL FePorMOF/GOx, 1.2 mM luminol, and 5 mM glucose was placed in a covered 96-well plate but not in the sealed PCR tube (used in Figure 1) for CL imaging; thus, the CL persistent time was slightly different from Figure 1. Although an obvious decrease of the duration time could be obtained after a storage of 19 days, the duration time of FePorMOF/GOx-glucose-luminol system was 340 min with a plateau period of 250 min even after a storage of 33 days (Figure 7A). In addition, the persistent CL trend of the FePorMOF/GOx-glucose-luminol system was kept during the whole storage period (Figure 7B). All of these results indicated the good catalytic stability of FePorMOF/GOx.

CL Imaging Assay of Glucose and AFP. The proposed FePorMOF/GOx-glucose-luminol system was used for CL imaging assay of glucose (Figure 8A). The CL intensity increased obviously with increasing the concentration of glucose, and a good linear correlation between the CL intensity and glucose concentration in the range from 50 to 1000 μM was obtained. The limit of detection (LOD) of glucose at 3SD was 39.2 μM.

https://dx.doi.org/10.1021/acs.analchem.0c00337
Anal. Chem. 2020, 92, 5517−5523

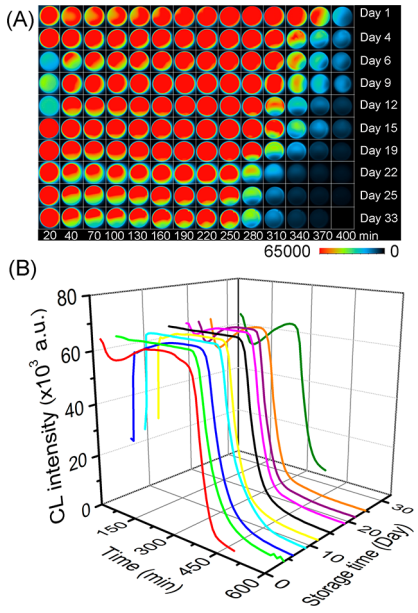

Figure 7. (A) CL imaging and (B) image intensity analysis of 0.1 mg/mL stored FePorMOF/GOx with 1.2 mM luminol and 5 mM glucose.

The results in Figure 6 showed both the FePorMOF/GOx-luminol-H_2O_2 and FePorMOF-GOx-glucose-luminol systems could generate CL emission more than 1 h due to the surface hindrance of FePorMOF and in situ H_2O_2 enzymatic production, respectively. Hence, we designed a FePorMOF/Ab1/BSA-GOx-luminol-glucose CL system for simple homogeneous CL imaging assay of AFP in which the detection was based on the sandwich immunoreaction-induced surface hindrance of FePorMOF and the CL system also kept the enzymatic generation of H_2O_2. In the presence of target, sandwich immunocomplexes were formed on the surface of FePorMOF, which hinder the diffusion of substrates including enzymatic produced H_2O_2 and luminol to the surface of FePorMOF,[39] resulting in the decrease of the CL intensity (Figure S4). The CL intensity and the logarithm of AFP concentration showed a linear relationship within 0.5−1000 ng/mL, with a correlation coefficient of 0.9554 (Figure 8B). Furthermore, due to its long-lasting CL characteristics, the real-time detection performance of the FePorMOF/Ab1/BSA-GOx-luminol-glucose CL immunoassay system was examined by continuous capture of CL intensity within 180 min (Figure S5). For all AFP concentrations, the CL intensity decreased gradually with time in the first 80 min, but after that, the CL intensity of AFP concentration higher than 10 ng/mL continued to decrease, while the CL intensity of AFP concentration less than or equal to 10 ng/mL showed a recovery. We speculated the turning point 80 min was the saturation immune time. After the complete immunoreaction on FePorMOF, the persistent CL performance could continue to occur in low AFP concentrations due to the small surface hindrance.

Finally, the specificity of the FePorMOF/Ab1/BSA-GOx-luminol-glucose CL immunoassay system was evaluated (Figure 8C). Compared with AFP, there was no significant change in CL intensity after adding BSA and thrombin, which indicated the proposed CL immunoassay had a good specificity for proteins. However, because this CL imaging immunoassay was based on the sandwich immunoreaction-induced surface diffusion inhibition, the detection of AFP in actual serum sample may not be very optimiztic. All-in-one CL probe which packaged GOx and CL substrate in FePorMOF would be developed in the follow-up experiment for immunoassay.

CONCLUSION

In summary, we have demonstrated an intensive and persistent CL system based on a nano-/bioenzymes conjugate of FePorMOF/GOx. FePorMOF nanozyme showed good peroxidase catalytic activity and environmental tolerance. The FePorMOF/GOx could generate strong CL emission over 9 h with glucose and luminol substrates due to its high catalytic efficiency based on the local tandem catalysis of CL reaction on the surface of FePorMOF. Importantly, a long constant CL emission of 7.5 h was observed for the first time in the FePorMOF/GOx-glucose-luminol system through controlling the CL reaction by in situ enzymatic H_2O_2 supply and substrate diffusion. In addition, the CL persistent time could be adjusted by luminol concentrations. Similarly, the long-lasting CL emission was also found in the FePorMOF/Ab1/BSA-GOx-luminol-glucose system. On the basis of the persistent CL system, a one-step homogeneous immunoassay was designed for continuous kinetic sensing of AFP. The proposed dual nano-/bioenzymes CL system, characterized with strong intensity, long constant emission, good stability, and physiological adaptation, showed potential applications in real-time bioassay and in vivo imaging.

ASSOCIATED CONTENT

Supporting Information

The Supporting Information is available free of charge at https://pubs.acs.org/doi/10.1021/acs.analchem.0c00337.

Kinetic parameters of FePorMOF and Fetcpp; FI-IR and PXRD characterization of FePorMOF; CL assay of H_2O_2; kinetic curves of the CL reaction; schematic

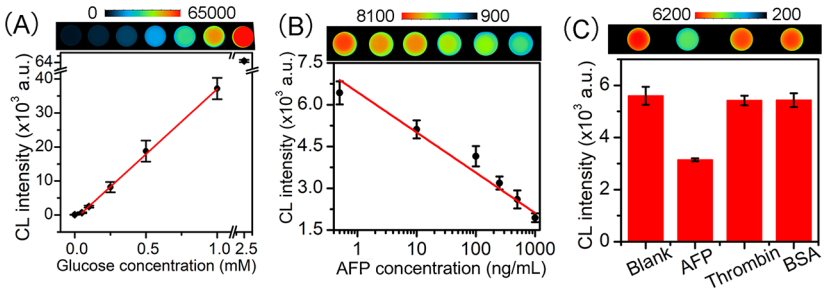

Figure 8. CL imaging assays of (A) glucose and (B) AFP and (C) specificity of AFP CL assay with 500 ng/mL AFP, BSA , and thrombin. Error bars were estimated from three parallel experiments.

https://dx.doi.org/10.1021/acs.analchem.0c00337
Anal. Chem. 2020, 92, 5517−5523

diagram of homogeneous CL imaging assay; continuous imaging assay of AFP (PDF)

AUTHOR INFORMATION

Corresponding Author

Jie Wu − *State Key Laboratory of Analytical Chemistry for Life Science, School of Chemistry and Chemical Engineering, Nanjing University, Nanjing 210023, People's Republic of China;* orcid.org/0000-0003-1379-122X; Phone: +86-25-89681923; Email: wujie@nju.edu.cn

Authors

Pengyun Dang − *State Key Laboratory of Analytical Chemistry for Life Science, School of Chemistry and Chemical Engineering, Nanjing University, Nanjing 210023, People's Republic of China*

Xuan Liu − *Medical Laboratory Center, The Second Hospital of Nanjing, Nanjing 210003, People's Republic of China*

Huangxian Ju − *State Key Laboratory of Analytical Chemistry for Life Science, School of Chemistry and Chemical Engineering, Nanjing University, Nanjing 210023, People's Republic of China;* orcid.org/0000-0002-6741-5302

Complete contact information is available at: https://pubs.acs.org/10.1021/acs.analchem.0c00337

Author Contributions

§P.D. and X.L. contributed equally to this work.

Notes

The authors declare no competing financial interest.

ACKNOWLEDGMENTS

We gratefully acknowledge the National Natural Science Foundation of China (Grant No. 21827812), and the Fundamental Research Funds for the Central Universities (Grant No. 2014380209).

REFERENCES

(1) Aslan, K.; Geddes, C. D. *Chem. Soc. Rev.* **2009**, *38*, 2556−2564.
(2) Liu, M. L.; Lin, Z.; Lin, J. M. *Anal. Chim. Acta* **2010**, *670*, 1−10.
(3) Lee, D.; Khaja, S.; Velasquez-Castano, J. C.; Dasari, M.; Sun, C.; Petros, J.; Taylor, W. R.; Murthy, N. *Nat. Mater.* **2007**, *6*, 765−769.
(4) Zhou, M.; Deng, L. Y.; Teng, Y. H.; Li, M. D.; Huang, X. Y.; Ren, J. C. *ACS Appl. Mater. Interfaces* **2019**, *2*, 3761−3768.
(5) Hananya, N.; Eldar Boock, A.; Bauer, C. R.; Satchi-Fainaro, R.; Shabat, D. R. *J. Am. Chem. Soc.* **2016**, *138*, 13438−13446.
(6) Li, J.; Zhao, X.; Chen, L. J.; Qian, H. L.; Wang, W. L.; Yang, C.; Yan, X. P. *Anal. Chem.* **2019**, *91*, 13191−13197.
(7) Xiao, Q.; Wu, J.; Dang, P. Y.; Ju, H. X. *Anal. Chim. Acta* **2018**, *1032*, 130−137.
(8) Hai, Z. J.; Li, J. D.; Wu, J. J.; Xu, J. C.; Liang, G. L. *J. Am. Chem. Soc.* **2017**, *139*, 1041−1044.
(9) Lee, Y. D.; Lim, C. K.; Singh, A.; Koh, J.; Kim, J.; Kwon, I. C.; Kim, S. *ACS Nano* **2012**, *6*, 6759−6766.
(10) Mao, D.; Wu, W.; Ji, S.; Chen, C.; Hu, F.; Kong, D.; Ding, D.; Liu, B. *Chem.* **2017**, *3*, 991−1007.
(11) Lim, C. K.; Lee, Y. D.; Na, J.; Oh, J. M.; Her, S.; Kim, K.; Choi, K.; Kim, S.; Kwon, I. C. *Adv. Funct. Mater.* **2010**, *20*, 2644−2648.
(12) Gnaim, S.; Scomparin, A.; Eldar-Boock, A.; Bauer, C. R.; Satchi-Fainaro, R.; Shabat, D. *Chem. Sci.* **2019**, *10*, 2945−2955.
(13) Son, S.; Won, M.; Green, O.; Hananya, N.; Sharma, A.; Jeon, Y.; Kwak, J. H.; Sessler, J. L.; Shabat, D.; Kim, J. S. *Angew. Chem., Int. Ed.* **2019**, *58*, 1739−1743.
(14) Roth-Konforti, M.; Green, O.; Hupfeld, M.; Fieseler, L.; Heinrich, N.; Ihssen, J.; Vorberg, R.; Wick, L.; Spitz, U.; Shabat, D. *Angew. Chem., Int. Ed.* **2019**, *58*, 10361−10367.
(15) Zhou, M.; Deng, L. Y.; Teng, Y. H.; Li, M. D.; Huang, X. Y.; Ren, J. C. *ACS Appl. Mater. Interfaces* **2019**, *2*, 3761−3768.
(16) Liu, Y. T.; Shen, W.; Cui, H. *Anal. Chem.* **2019**, *91*, 10614−10621.
(17) Liu, Y. T.; Shen, W.; Li, Q.; Shu, J. N.; Gao, L. F.; Ma, M. M.; Wang, W.; Cui, H. *Nat. Commun.* **2017**, *8*, 1003.
(18) Xue, T.; Peng, B.; Xue, M.; Zhong, X.; Chiu, C. Y.; Yang, S.; Qu, Y. Q.; Ruan, L. Y.; Jiang, S.; Dubin, S.; Kaner, R. B.; Zink, J. I.; Meyerhoff, M. E.; Duan, X. F.; Huang, Y. *Nat. Commun.* **2014**, *5*, 3200.
(19) Kim, C. K.; Kim, T.; Choi, I. Y.; Soh, M.; Kim, D.; Kim, Y. J.; Jang, H.; Yang, H. S.; Kim, J. Y.; Park, H. K.; Park, S. P.; Park, S.; Yu, T.; Yoon, B. W.; Lee, S. H.; Hyeon, T. *Angew. Chem., Int. Ed.* **2012**, *51*, 11039−11043.
(20) Wei, H.; Wang, E. *Anal. Chem.* **2008**, *80*, 2250−2254.
(21) Luo, F. Q.; Lin, Y. L.; Zheng, L. Y.; Lin, X. M.; Chi, Y. W. *ACS Appl. Mater. Interfaces* **2015**, *7*, 11322−11329.
(22) Li, J. R.; Sculley, J.; Zhou, H. C. *Chem. Rev.* **2012**, *112*, 869−932.
(23) Horcajada, P.; Gref, R.; Baati, T.; Allan, P. K.; Maurin, G.; Couvreur, P.; Ferey, G.; Morris, R. E.; Serre, C. *Chem. Rev.* **2012**, *112*, 1232−1268.
(24) Kreno, L. E.; Leong, K.; Farha, O. K.; Allendorf, M.; Van Duyne, R. P.; Hupp, J. T. *Chem. Rev.* **2012**, *112*, 1105−1125.
(25) Suh, M. P.; Park, H. J.; Prasad, T. K.; Lim, D. W. *Chem. Rev.* **2012**, *112*, 782−835.
(26) Yang, N.; Song, H. J.; Wan, X. Y.; Fan, X. Q.; Su, Y. Y.; Lv, Y. *Analyst* **2015**, *140*, 2656−2663.
(27) Yi, X. L.; Dong, W. F.; Zhang, X. D.; Xie, J. X.; Huang, Y. M. *Anal. Bioanal. Chem.* **2016**, *408*, 8805−8812.
(28) Yu, H. L.; Long, D. Y. *Microchim. Acta* **2016**, *183*, 3151−3157.
(29) Zhao, Z.; Fu, J. L.; Dhakal, S.; Johnson-Buck, A.; Liu, M. H.; Zhang, T.; Woodbury, N. W.; Liu, Y.; Walter, N. G.; Yan, H. *Nat. Commun.* **2016**, *7*, 10619.
(30) Liu, Y.; Du, J. J.; Yan, M.; Lau, M. Y.; Hu, J.; Han, H.; Yang, O. O.; Liang, S.; Wei, W.; Wang, H.; Li, J. M.; Zhu, X. Y.; Shi, L. Q.; Chen, W.; Ji, C.; Lu, Y. F. *Nat. Nanotechnol.* **2013**, *8*, 187−192.
(31) Cheng, H. J.; Zhang, L.; He, J.; Guo, W. J.; Zhou, Z. Y.; Zhang, X. J.; Nie, S. M.; Wei, H. *Anal. Chem.* **2016**, *88*, 5489−5497.
(32) Xu, S. X.; Li, X. M.; Li, C. B.; Li, J. L.; Zhang, X. F.; Wu, P.; Hou, X. D. *Anal. Chem.* **2016**, *88*, 6418−6424.
(33) Ling, P. H.; Lei, J. P.; Ju, H. X. *Anal. Chem.* **2016**, *88*, 10680−10686.
(34) Wang, Q. G.; Yang, Z. M.; Zhang, X. Q.; Xiao, X. D.; Chang, C. K.; Xu, B. *Angew. Chem., Int. Ed.* **2007**, *46*, 4285−4289.
(35) Xue, T.; Jiang, S.; Qu, Y. Q.; Su, Q.; Cheng, R.; Dubin, S.; Chiu, C. Y.; Kaner, R.; Huang, Y.; Duan, X. F. *Angew. Chem., Int. Ed.* **2012**, *51*, 3822−3825.
(36) Yamaguchi, H.; Tsubouchi, K.; Kawaguchi, K.; Horita, E.; Harada, A. *Chem. - Eur. J.* **2004**, *10*, 6179−6186.
(37) Merenyi, G.; Lind, J. S. *J. Am. Chem. Soc.* **1980**, *102*, 5830−5835.
(38) Lian, X. Z.; Chen, Y. P.; Liu, T. F.; Zhou, H. C. *Chem. Sci.* **2016**, *7*, 6969−6973.
(39) Yang, Z. J.; Cao, Y.; Li, J.; Lu, M. M.; Jiang, Z. K.; Hu, X. Y. *ACS Appl. Mater. Interfaces* **2016**, *8*, 12031−12038.

https://dx.doi.org/10.1021/acs.analchem.0c00337
Anal. Chem. 2020, 92, 5517−5523